Radiation-induced direct bandgap transition in few-layer MoS_2

Bo Wang, Sisi Yang, Jihan Chen, Colin Mann, Adam Bushmaker, and Stephen B. Cronin

Citation: Appl. Phys. Lett. **111**, 131101 (2017); doi: 10.1063/1.5005121
View online: http://dx.doi.org/10.1063/1.5005121
View Table of Contents: http://aip.scitation.org/toc/apl/111/13
Published by the American Institute of Physics

Radiation-induced direct bandgap transition in few-layer MoS_2

Bo Wang,[1] Sisi Yang,[1] Jihan Chen,[2] Colin Mann,[3] Adam Bushmaker,[3] and Stephen B. Cronin[1,2]
[1]*Department of Physics and Astronomy, University of Southern California, Los Angeles, California 90089, USA*
[2]*Ming Hsieh Department of Electrical Engineering, University of Southern California, Los Angeles, California 90089, USA*
[3]*Physical Sciences Laboratories, The Aerospace Corporation, 355 S. Douglas Street, El Segundo, California 90245, USA*

(Received 22 May 2017; accepted 16 September 2017; published online 27 September 2017)

We report photoluminescence (PL) spectroscopy of air-suspended and substrate-supported molybdenum disulfide (MoS_2) taken before and after exposure to proton radiation. For 2-, 3-, and 4-layer MoS_2, the radiation causes a substantial ($>10\times$) suppression of the indirect bandgap emission, likely due to a radiation-induced decoupling of the layers. For all samples measured (including the monolayer), we see the emergence of a defect-induced shoulder peak at around 1.7 eV, which is redshifted from the main direct bandgap emission at 1.85 eV. Here, defects induced by the radiation trap the excitons and cause them to be redshifted from the main direct band emission. After annealing, the defect-induced sideband disappears, but the indirect band emission remains suppressed, indicating a permanent transition into a direct bandgap material. While suspended 2-, 3-, and 4-layer MoS_2 show no change in the intensity of the direct band emission after radiation exposure, substrate-supported MoS_2 exhibits an approximately 2-fold increase in the direct bandgap emission after irradiation. Suspended monolayer MoS_2 shows a $2–3\times$ drop in PL intensity; however, substrate-supported monolayer MoS_2 shows a 2-fold increase in the direct band emission. *Published by AIP Publishing*. https://doi.org/10.1063/1.5005121

Radiation effects can severely and negatively impact the performance of microelectronic and optoelectronic devices operating in high radiation environments, such as near particle accelerators, and in space radiation environments. Radiation induced displacement damage is particularly harmful for minority carrier devices such as optoelectronic components, diodes, and bipolar junction transistors (BJTs), where lattice defects can provide non-radiative decay pathways, greatly reducing the minority carrier lifetime.[1] This is of particular concern for direct bandgap 2D semiconductors, such as MoS_2, due to the interest in these materials for optoelectronic applications. Also, radiation-induced charging of insulators in close proximity to semiconductor materials can induce unintentional changes in the carrier density due to the field effect. This is of concern because 2D semiconductors are typically supported on insulating substrates when used as the channel material in advanced field effect transistors (FETs).[2] From a fundamental scientific perspective, we can conclude that these low dimensional materials provide a good platform for studying the effects of radiation due to their high surface-to-volume ratio and the unique physics associated with indirect-to-direct bandgap transitions, excitons, and trions.[3,4]

In addition to studying the effects of energetic particle radiation, it is worth noting that energetic particles are commonly used for surface treatment in the semiconductor industry. For example, plasma treatments are used to improve material surface wettability and bonding, surface functionalization, and material etching and doping. In the work presented here, we report the effects of radiation exposure that improve the optoelectronic properties of multi-layer MoS_2 by inducing an indirect-to-direct bandgap transition and, thereby, increasing the PL efficiency of the material.

There have been several studies on the effects of radiation on the electronic properties of 2D materials. Kim *et al.* studied the effects of proton radiation on MoS_2 FETs and observed a substantial decrease in the conductance as well as shifts in the threshold voltage after irradiation.[5] Zhang *et al.* reported the effects of X-ray irradiation on similar back-gated MoS_2 transistors, which resulted in decreased conductance and substantial shifts in the threshold voltage.[6] Lee and coworkers studied the effects of 662 keV γ-radiation on suspended MoS_2 micromechanical resonators and found that charges induced by the radiation caused a frequency upshift of 2% of the resonance frequency.[7] The radiation hardness of MoS_2 FETs was investigated by Ochedowski with 1.14 GeV U^{28+} ions, and significant changes in the structural and electrical properties were observed by electrical characterization, atomic force microscopy (AFM), and Raman spectroscopy.[8] Tsai *et al.* showed that trilayer MoS_2 metal-semiconductor-metal photodetectors exhibit high responsivity ($\sim$1.04 A/W) and photogain and are stable under 2 MeV proton illumination radiation, indicating that they can be used in harsh environments.[9] Zan *et al.* demonstrated that electron beam radiation damage of MoS_2 flakes can be mitigated by encapsulation in graphene.[10] While these previous studies have focused on the electronic properties of irradiated MoS_2, there have been few reports on the optoelectronic properties after irradiation. Tongay *et al.* investigated the effects of α-particle radiation on substrate-supported, monolayer MoS_2.[11] In this previous work, they observed defect-activated photoluminescence and a blue shift in the direct

transition PL peak after irradiation, as described by the interplay between bound and free excitons. However, to date, there have been no reports on the effects of energetic particle radiation on PL from multi-layer 2D semiconductors or suspended monolayer 2D semiconductors. Several other groups have studied the effect of ion irradiation on 2D materials both theoretically and experimentally.[12–17] However, none of these previous studies discuss an indirect-to-direct bandgap transition.

In the work presented here, we study the effects of proton radiation on the optoelectronic properties of MoS_2. The PL spectra give sensitive information about the changes in the band structure (i.e., indirect-to-direct bandgap) and defects through the suppression of the indirect 1.4 eV peak and defect-induced sidebands. We study the radiation effects on both suspended and substrate-supported MoS_2, for a variety of different thicknesses. Post-radiation annealing is also performed in order to investigate the nature of the defects. By investigating the suspended material alongside the substrate-supported material, we are able to understand the fundamental changes in the optical properties of the material without substrate perturbation and also independently understand the influence of the substrate.

Exfoliated MoS_2 flakes are transferred to 20 μm wide silicon nitride membranes containing several holes approximately 2–3 μm in size, as shown in Fig. 1. Here, MoS_2 is first exfoliated onto transparent polydimethylsiloxane (PDMS) substrates. Once a flake of the desired thickness is located, the flake is then transferred to one of the "hole" regions in the SiN membrane using a home built contact aligner (i.e., dry transfer method) with a 50× objective lens.[18] PL spectra were collected from both suspended and non-suspended regions of MoS_2 using a Renishaw *InVia* micro-spectrometer using 532 nm wavelength light before and after proton irradiation. The thickness of the flakes is determined from the contrast in the optical microscopy images and the energy of the indirect band emission peak in the PL spectra.[19,20] Scanning electron microscopy (SEM) images were taken after all optical characterization, in order to avoid contamination and potential quenching of the MoS_2 photoluminescence. Figure 1 shows optical microscopy and SEM images of one of the flakes investigated in this study. No visible differences in the sample can be seen in the optical or electron microscopy after irradiation.

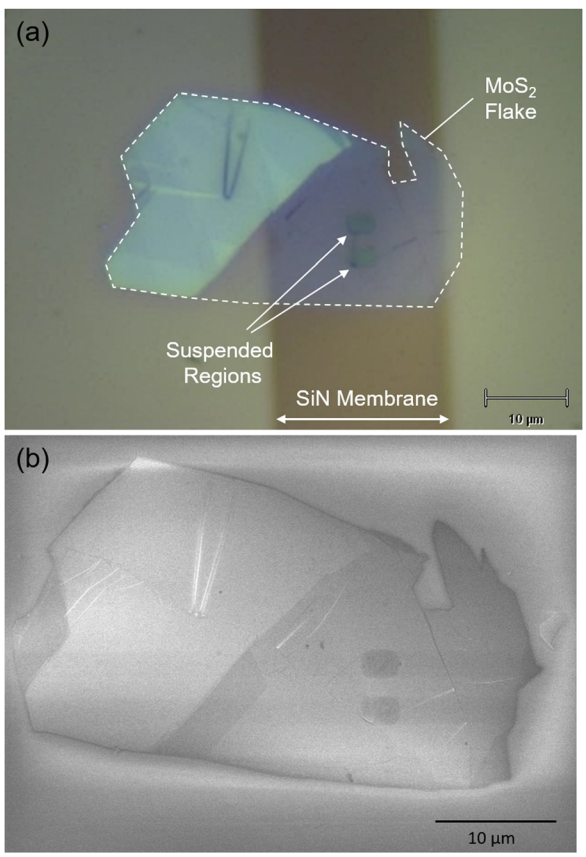

FIG. 1. (a) Optical microscopy and (b) SEM image of an MoS_2 flake deposited on a SiN membrane. Two holes in this membrane provide a suspended region of the flake to measure, which behave quite differently from the substrate-supported region.

The LEAF (Low Energy Accelerator Facility) contains a 400 keV ion accelerator capable of producing beam currents from 10 pA up to 1 mA. Its primary use is implanting with protons (H^+) although other heavier ions are also possible. Here, we focus on energetic protons since they are the most common type of space radiation and thus allow us to best evaluate the effect caused by exposure of this material to the space radiation environment. Using a scanned particle beam, the system delivers fluences as low as 1×10^9 up to 1×10^{17} particles/cm^2. For the MoS_2 irradiations, we irradiate at 100 keV with fluences ranging from 2×10^{12} to 6×10^{14} particles/cm^2. Here, the radiation beam aperture (1″) is larger than the sample (3 mm). Using a beam current of 1 μA at a flux of ∼10 nA/cm^2, the sample shows an incoming power of 1mW from the beam during irradiation. The low power of the particle beam eliminates the need for cooling of the sample during irradiation.

Figure 2 shows the PL spectra of a bilayer flake measured before and after irradiation with a fluence of 6×10^{14} protons/cm^2. Several PL spectra were collected from each sample, which exhibited a high degree of uniformity. Each of these spectra was fitted with three Lorentzian peaks, and the details of these fits are given in the supplementary material. Here, a Lorentzian function provides better fits to the spectra than a Gaussian. Both the suspended and substrate-supported regions show almost complete suppression of the indirect emission (1.55–1.6 eV) after irradiation and the emergence of a defect-induced sideband peak at around 1.7 eV. Here, defects induced by the radiation trap the excitons and cause them to be redshifted from the main direct band emission at 1.83 eV. In the suspended region, the direct band emission at 1.83 eV increases by 1.6× after irradiation, while the substrate-supported direct band emission increases by a factor of 2.7×. After annealing the samples at 300 °C for 1 h in argon, the defect-induced sideband peak disappears. However, the indirect band emission remains suppressed after annealing, indicating that the material has undergone an irreversible indirect-to-direct bandgap transition. These measurements were repeated on several other bilayer flakes (shown in the supplementary material), and the same results were consistently observed. Here, we believe that the proton irradiation causes a slight decoupling of the layers, as we have previously observed using an oxygen plasma treatment.[4] The density functional theory (DFT)

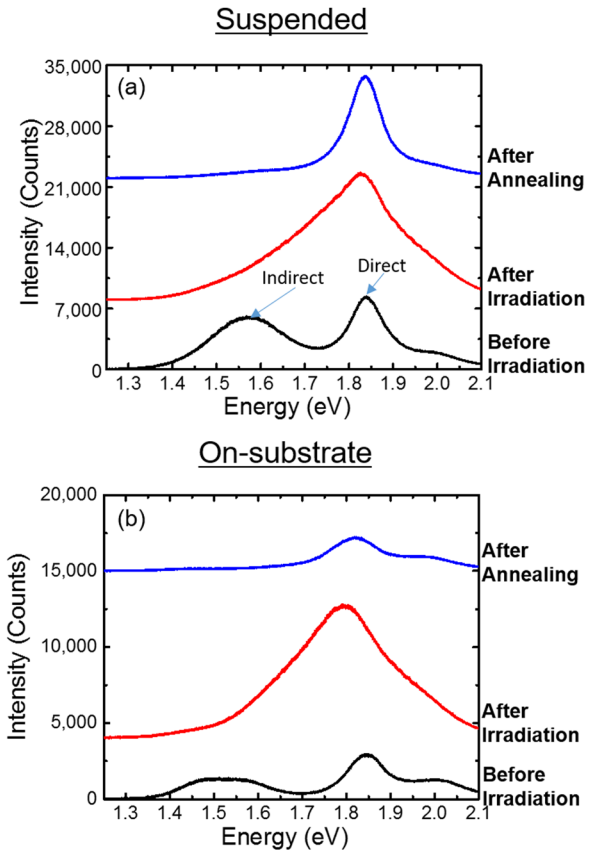

FIG. 2. PL spectra of bilayer MoS_2 taken before and after proton irradiation, and after annealing.

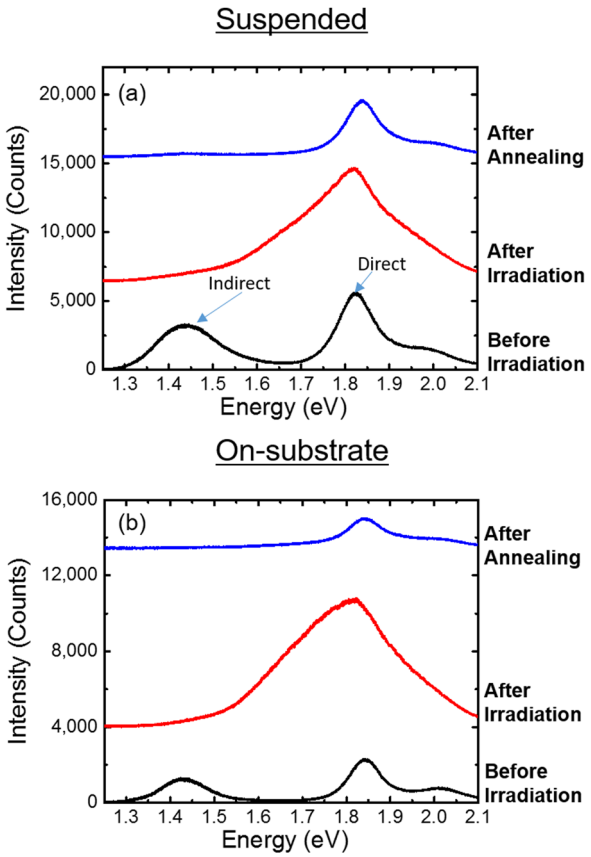

FIG. 3. PL spectra of trilayer MoS_2 taken before and after proton irradiation, and after annealing.

calculations by Lake and coworkers established that an increase in the interlayer separation of just 1 Å is sufficient to induce an indirect-to-direct bandgap transition in this material,[4] which was confirmed experimentally with AFM measurements.[4] While these DFT calculations provide a qualitative explanation of the mechanism underlying this indirect-to-direct bandgap transition, we do not currently have an atomistic picture of the ion interaction with the lattice of this material. The suppression of the indirect bandgap emission is potentially useful for fabricating optoelectronic devices such as LEDs and solar cells. Spectra taken after an intermediate proton fluence of 6×10^{13} protons/cm^2 and a heavier fluence of 6×10^{15} protons/cm^2 are also shown in the supplementary material. For the heaviest fluence, the PL intensity decreases, indicating that the effects of radiation-induced defects eventually outweigh the indirect-to-direct bandgap transition.

Figures 3 and 4 show MoS_2 samples with 3 or more layers in thickness (after irradiation and before annealing), which, again, show slightly enhanced direct bandgap emission, complete suppression of the indirect emission at around 1.4 eV, and a broadened, red-shifted defect induced sideband at around 1.7 eV. In addition, the spectra of suspended multi-layer MoS_2 look very similar to those of substrate-supported multi-layer MoS_2 (See Fig. S12 in the supplementary material), reflecting the decreased sensitivity to substrate interactions as the material approaches the bulk limit. After annealing, the indirect emission remains suppressed, indicating that an indirect-to-direct bandgap transition is stable against annealing at 300 °C. Also, the defect-induced sideband

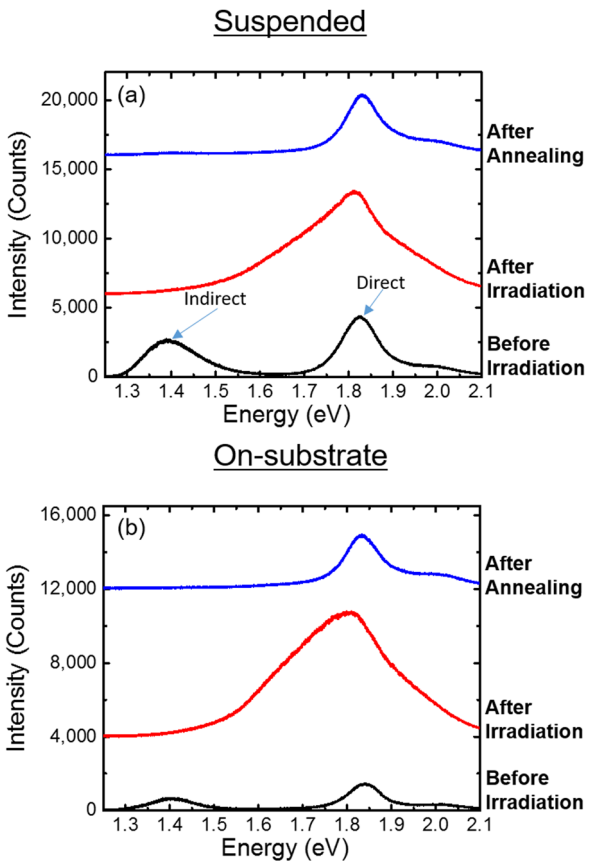

FIG. 4. PL spectra of MoS_2 with four layers taken before and after proton irradiation, and after annealing.

disappears and the direct emission decreases to roughly their pre-radiation intensities after annealing. The detailed fits of these spectra are given in the supplementary material, along with additional datasets measured on other multilayer flakes, showing that the same behavior is observed consistently.

Figure 5 shows the PL spectra of a monolayer MoS_2 flake measured before and after irradiation with a fluence of 6×10^{14} protons/cm^2. These monolayer data serve a good control group, showing the material's response to changes in the defect concentration without corresponding changes in the band structure. Again, each of these spectra was fitted with three peaks, as shown in the supplementary material. In the suspended region, we see a 2-fold drop in the intensity of the direct bandgap emission after irradiation and the emergence of a defect-induced sideband peak at 1.71 eV. As mentioned above, defects induced by the radiation trap the excitons and cause them to be redshifted from the main direct band emission at 1.85 eV. For the suspended region, we understand this decrease in intensity due to defects, which cause non-radiative recombination and shorten the lifetime of the photoexcited carriers. Under all conditions, the PL intensity in the substrate-supported region of the MoS_2 is much weaker than that in the suspended region, as shown in Fig. S8 of the supplementary material, consistent with the original reports of Mak *et al.*[19] Here, we see a 2× increase in the direct bandgap emission at 1.85 eV for the substrate-supported region after irradiation. As with the suspended region, we observe an increase in the defect-induced peak at around 1.7 eV, as was reported by Tongay *et al.*[11] After annealing the samples at 300 °C for 1 h in argon, the defect-induced sideband peak disappears in the suspended region and is reduced by 5× in the substrate supported region. Also, the direct band emission reverts back to its original pre-irradiated intensity, indicating that we can fully restore the material to its original state by annealing the defects. These measurements were repeated on several other monolayer flakes (shown in the supplementary material), and the same results were consistently observed. Spectra taken after an intermediate proton fluence of 6×10^{13} protons/cm^2 are also shown in the supplementary material. Spectra taken at a fluence of 6×10^{13} protons/cm^2 can be compared with the PL results reported by Tongay *et al.*,[11] who reported PL spectra of MoS_2 exposed to 5×10^{13} particles/cm^2 for 3.04 MeV α-particle radiation, which have similar stopping power (i.e., deposit a similar energy per path length) compared to the 100 keV protons using in the work reported here.

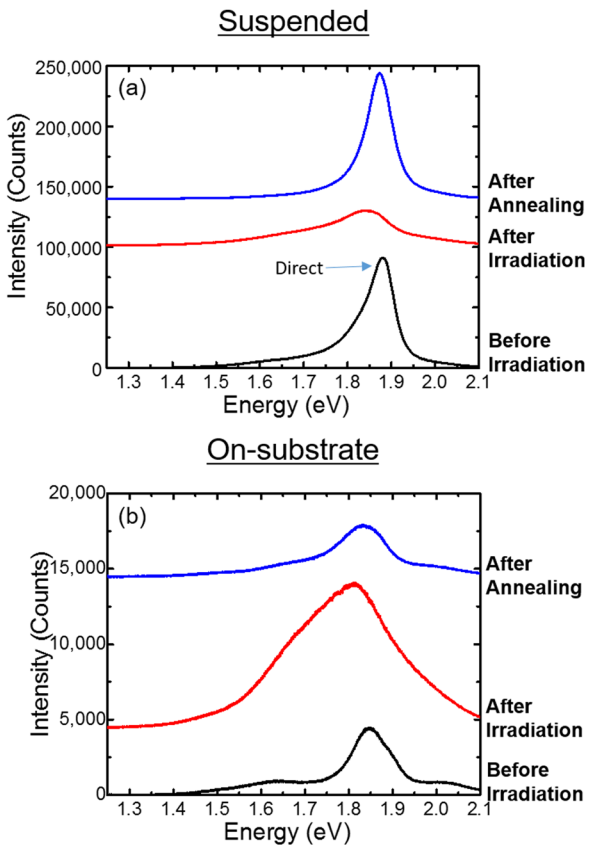

FIG. 5. PL spectra of monolayer MoS_2 taken before and after proton irradiation, and after annealing.

In summary, we demonstrate enhanced photoluminescence and direct bandgap emission in proton irradiated MoS_2 flakes. For all substrate-supported samples and most of the suspended samples, the PL intensity increased after irradiation and the indirect emission is almost completely suppressed, due to decoupling of the layers (i.e., direct-to-indirect transition). In all samples measured, we see the emergence of a defect-induced sideband peak at around 1.7 eV, which can be annealed out by heating the samples to 300 °C. Only suspended monolayer MoS_2 shows a decrease in the PL intensity by a factor of 2.8×, likely due to the creation of defects and recombination centers. Perhaps the most interesting finding is that, after annealing, the indirect emission remains completely suppressed, indicating that this is a robust way to convert this material from an indirect bandgap semiconductor into a direct bandgap semiconductor.

See supplementary material for additional experimental data including Raman spectra and heavy dose radiation results.

This research was supported by the NSF Award No. 1402906 (B.W.) and the Department of Energy DOE Award No. DE-FG02-07ER46376 (J.C.). The authors would also like to acknowledge support from the Northrop Grumman-Institute of Optical Nanomaterials and Nanophotonics (NG-ION^2) (S.Y.). The portion of the work done at The Aerospace Corporation was funded by the independent research and development program at the Aerospace Corporation.

[1]G. F. Knoll, *Radiation Detection and Measurement*, 4th ed. (Wiley, Hoboken, NJ, 2010).
[2]R. Dhall, Z. Li, E. Kosmowska, and S. B. Cronin, J. Appl. Phys. **120**(19), 195702 (2016).
[3]J. S. Ross, S. F. Wu, H. Y. Yu, N. J. Ghimire, A. M. Jones, G. Aivazian, J. Q. Yan, D. G. Mandrus, D. Xiao, W. Yao, and X. D. Xu, Nat. Commun. **4**, 1474 (2013).
[4]R. Dhall, M. R. Neupane, D. Wickramaratne, M. Mecklenburg, Z. Li, C. Moore, R. K. Lake, and S. Cronin, Adv. Mater. **27**(9), 1573 (2015).
[5]T. Y. Kim, K. Cho, W. Park, J. Park, Y. Song, S. Hong, W. K. Hong, and T. Lee, ACS Nano **8**(3), 2774–2781 (2014).
[6]C. X. Zhang, A. K. M. Newaz, B. Wang, E. X. Zhang, G. X. Duan, D. M. Fleetwood, M. L. Alles, R. D. Schrimpf, K. I. Bolotin, and S. T. Pantelides, IEEE Trans. Nucl. Sci. **61**(6), 2862–2867 (2014).
[7]J. Lee, M. J. Krupcale, and P. X. L. Feng, Appl. Phys. Lett. **108**(2), 023106 (2016).

[8]O. Ochedowski, K. Marinov, G. Wilbs, G. Keller, N. Scheuschner, D. Severin, M. Bender, J. Maultzsch, F. J. Tegude, and M. Schleberger, J. Appl. Phys. **113**(21), 214306 (2013).
[9]D. S. Tsai, D. H. Lien, M. L. Tsai, S. H. Su, K. M. Chen, J. J. Ke, Y. C. Yu, L. J. Li, and J. H. He, IEEE J. Sel. Top. Quantum Electron. **20**(1), 30–35 (2014).
[10]R. Zan, Q. M. Ramasse, R. Jalil, T. Georgiou, U. Bangert, and K. S. Novoselov, ACS Nano **7**(11), 10167–10174 (2013).
[11]S. Tongay, J. Suh, C. Ataca, W. Fan, A. Luce, J. S. Kang, J. Liu, C. Ko, R. Raghunathanan, J. Zhou, F. Ogletree, J. B. Li, J. C. Grossman, and J. Q. Wu, Sci. Rep. **3**, 2657 (2013).
[12]D. S. Fox, Y. B. Zhou, P. Maguire, A. O'Neill, C. O'Coileain, R. Gatensby, A. M. Glushenkov, T. Tao, G. S. Duesberg, I. V. Shvets, M. Abid, M. Abid, H. C. Wu, Y. Chen, J. N. Coleman, J. F. Donegan, and H. Z. Zhang, Nano Lett. **15**(8), 5307–5313 (2015).
[13]M. Ghorbani-Asl, S. Kretschmer, D. E. Spearot, and A. V. Krasheninnikov, 2D Mater. **4**(2), 025078 (2017).
[14]Z. Lin, B. R. Carvalho, E. Kahn, R. T. Lv, R. Rao, H. Terrones, M. A. Pimenta, and M. Terrones, 2D Mater. **3**(2), 022002 (2016).
[15]Q. Ma, P. M. Odenthal, J. Mann, D. Le, C. S. Wang, Y. M. Zhu, T. Y. Chen, D. Z. Sun, K. Yamaguchi, T. Tran, M. Wurch, J. L. McKinley, J. Wyrick, K. Magnone, T. F. Heinz, T. S. Rahman, R. Kawakami, and L. Bartels, J. Phys. Condens. Matter **25**(25), 252201 (2013).
[16]K. C. Santosh, R. C. Longo, R. Addou, R. M. Wallace, and K. Cho, Nanotechnology **25**(37), 375703 (2014).
[17]N. Scheuschner, O. Ochedowski, A. M. Kaulitz, R. Gillen, M. Schleberger, and J. Maultzsch, Phys. Rev. B **89**(12), 125406 (2014).
[18]R. Yang, X. Q. Zheng, Z. H. Wang, C. J. Miller, and P. X. L. Feng, J. Vacuum Sci. Technol. B **32**(6), 061203 (2014).
[19]K. F. Mak, C. Lee, J. Hone, J. Shan, and T. F. Heinz, Phys. Rev. Lett. **105**(13), 136805 (2010).
[20]J. Park, N. Choudhary, J. Smith, G. Lee, M. Kim, and W. Choi, Appl. Phys. Lett. **106**(1), 012104 (2015).